

PAPER • OPEN ACCESS

## An investigation of the generalized model of pyroelectric thermal IR detectors

To cite this article: A V Popov *et al* 2019 *J. Phys.: Conf. Ser.* **1400** 066060

View the [article online](#) for updates and enhancements.



**IOP | ebooks™**

Bringing you innovative digital publishing with leading voices to create your essential collection of books in STEM research.

Start exploring the collection - download the first chapter of every title for free.

# An investigation of the generalized model of pyroelectric thermal IR detectors

A V Popov<sup>1</sup> \*, E A Ilyichev<sup>1</sup>\*\* and G D Demin<sup>1,2</sup> \*\*\*

<sup>1</sup> National Research University of Electronic Technology (MIET), Id. 1, Shokin Square, 124498, Zelenograd, Moscow, Russia

<sup>2</sup> Moscow Institute of Physics and Technology (State University), 9 Institutskiy per., 141701, Dolgoprudny, Moscow, Russia

E-mail: \* alexcoretex@gmail.com, \*\*egil44@mail.ru, \*\*\* gddemin@edu.miet.ru

**Abstract.** In our work, a compact model of an infrared radiation detector based on a LiTaO<sub>3</sub> pyroelectric material (lithium tantalate) is presented. Based on the developed model, the time-dependent characteristics of the pyroelectric current, voltage and the surface temperature of such detector were calculated. The obtained results can be used in the development of detectors of thermal images of objects operating in the wavelength range from 3 to 15  $\mu\text{m}$ .

## 1. Introduction

The systems for contactless detection of thermal images are widely used in various fields of human activity [1]. The principle of operation of these devices is the detection of thermal radiation from the investigated body with a special material that is sensitive to this radiation.

Progress in the development of infrared (IR) radiation receivers of the long-wave spectrum directly depends on the fulfillment of the following three key tasks: 1) increasing the signal-to-noise ratio, 2) enabling the receiver to work at room temperature, and 3) achieving spatial resolution acceptable for applied tasks [2, 3].

During the search for physical principles and materials for detecting images in a given spectral range, materials were discovered that have spontaneous polarization, the magnitude of which depends on temperature. Such materials began to be called as pyroelectrics.

One of the most interesting types of pyroelectric materials is ferroelectrics, which has the highest sensitivity to IR radiation [4]. It should be noted that all ferroelectrics possess the properties of pyroelectrics. However, these properties appear only at temperatures below the Curie temperature.

## 2. Basic equations

### 2.1. Pyroelectric coefficient

The pyroelectric effect consists of the total contribution of the primary and secondary pyroelectric effects:

- to describe the primary pyroelectric effect, which characterizes the disordering of dipoles when the temperature of the pyroelectric varies (at temperatures  $T \ll T_C$ ), a primary pyroelectric coefficient  $p_l$  is introduced as the ratio of the amplitude of the spontaneous polarization vector  $\Delta P_l$  to the temperature change  $\Delta T$  of the pyroelectric material [5]:



$$\Delta P_I = p_I \Delta T \quad (1)$$

• to describe the secondary pyroelectric effect, which characterizes the piezoelectric contribution from the thermal expansion of a pyroelectric, a secondary pyroelectric coefficient  $p_{II}$  is introduced in the form of a product of the piezoelectric coefficient  $\zeta$  and thermal expansion coefficient  $\alpha$  [6]:

$$\Delta P_{II} = \zeta \alpha \Delta T = p_{II} \Delta T \quad (2)$$

Thus, the total pyroelectric effect is represented as the sum of the primary and secondary pyroelectric effects, correspondingly:

$$\Delta P_{\Sigma} = \Delta P_I + \Delta P_{II} \quad (3)$$

Hence, the total pyroelectric coefficient will be represented in the form:

$$p_{\Sigma} = p_I + p_{II}, \quad (4)$$

where the coefficient  $p_{\Sigma}$  can be estimated experimentally for the material of interest to us. In particular, the value of the total pyroelectric coefficient for LiTaO<sub>3</sub> is  $p_{\Sigma} = -176 \mu C / m^2 K$  (see the data of reference tables in [7]).

## 2.2. Pyroelectric temperature

To calculate the temperature of the pyroelectric, the heat balance equation [8] was used, which is valid for relatively thin films (having a thickness  $d < 10 \mu m$ ):

$$C_{th} \frac{d(\Delta T)}{dt} + G_{th} \Delta T = \eta \Phi, \quad (5)$$

where  $\Phi$  is the surface power density of the heat flux from the heated object being detected,  $\eta$  is the absorption coefficient of incident radiation,  $C_{th}$  is the heat capacity,  $G_{th}$  is the thermal conductivity and  $\Delta T$  is the pyroelectric temperature change.

The solution of equation (5), without taking into account the modulation of radiation, will be the analytical function  $\Delta T(t)$ :

$$\Delta T(t) = \frac{\eta \Phi}{G_{th}} \{1 - \exp(-G_{th} t / C_{th})\} \quad (6)$$

When describing the input surface density of thermal radiation, the Stefan-Boltzmann equation is used:

$$\Phi = \varepsilon \sigma (T_O^4 - T_R^4), \quad (7)$$

where  $\varepsilon$  is the emissivity,  $\sigma$  is the Stefan-Boltzmann constant,  $T_O$  is the heated object temperature,  $T_R$  is the room temperature (ambient temperature).

Our model takes into account the heat loss of the pyroelectric material due to radiation through the component  $G_{Stefan-Boltzmann}$  involved in the total thermal conductivity of the pyroelectric:

$$G_{th} = G_{pyro} + G_{Stefan-Boltzmann} = G_{pyro} + 4S\varepsilon\sigma T_{pyro}^3, \quad (8)$$

where  $G_{pyro}$  is the thermal conductivity of the pyroelectric material,  $S$  is the pyroelectric surface area,  $T_{pyro}$  is the pyroelectric temperature.

We will further assume in our simulation that  $S = 1.5 \times 1.5 cm^2 = 2.25 cm^2$ .

## 2.3. Pyroelectric voltage and pyroelectric current

When the temperature of the pyroelectric changes by  $\Delta T$  during heating, the amplitude of the spontaneous polarization vector also changes by  $\Delta P$ , which leads to a redistribution of charges on the

pyroelectric surface. The surface charge  $\Delta Q$  created by the spontaneous polarization  $\Delta P$  creates a surface potential  $\Delta V$ , which, in turn, can be simply calculated in the case of considering the IR radiation receiver as a flat capacitor with a capacitance  $C$ :

$$\Delta Q = \Delta PS \quad (9)$$

Then, we get the next expression for the induced pyroelectric voltage:

$$\Delta V = \frac{\Delta Q}{C} = \frac{\Delta PS}{\left(\frac{\varepsilon\varepsilon_0 S}{d}\right)} = \frac{\Delta Pd}{\varepsilon\varepsilon_0} \quad (10)$$

Taking into account (1-4), equation (10) can be represented as:

$$\Delta V = \frac{\Delta Pd}{\varepsilon\varepsilon_0} = \frac{p_\Sigma \Delta T d}{\varepsilon\varepsilon_0} \quad (11)$$

From equation (11) it follows that the ratio of the pyroelectric potential  $\Delta V$  to the temperature change  $\Delta T$  at temperatures  $T \ll T_C$  is a constant value:

$$\frac{\Delta V}{\Delta T} = \frac{p_\Sigma d}{\varepsilon\varepsilon_0} = const \quad (12)$$

Thus, the criteria for selecting the optimal pyroelectric parameters for the implementation of the maximum value of the pyroelectric voltage include:

- 1) the choice of material with the highest pyroelectric coefficient;
- 2) the choice of pyroelectric material with low dielectric constant;
- 3) optimization of pyroelectric film thickness.

The pyroelectric current was calculated as the limit of ratio of the charge change  $\Delta Q$  to the time interval  $\Delta t$ :

$$I = \lim_{\Delta t \rightarrow 0} \frac{\Delta Q}{\Delta t} = \frac{dQ}{dt} = S \frac{dP}{dt} = p_\Sigma S \frac{dT}{dt} \quad (13)$$

### 3. Pyroelectric model

The pyroelectric model developed using Matlab Simulink software consists of two parts:

- 1) Function for calculating the temperature change of a pyroelectric film over time based on the solution of equation (5);
- 2) Function for calculating the time-dependent characteristics of the pyroelectric voltage and current, based on equations (5), (11) and (13).

A block diagram of the algorithm of pyroelectric model is presented in Figure 1.

The parameters of the pyroelectric  $\text{LiTaO}_3$  used in the simulation are shown in Table 1 [9, 10]:

**Table 1.**  $\text{LiTaO}_3$  parameters

	$S$ ( $\text{cm}^2$ )	$d$ ( $\mu\text{m}$ )	$e$	$P_{total}$ ( $\mu\text{C}/(\text{m}^2 \cdot \text{K})$ )	$G_{th}$ ( $\text{W}/(\text{m} \cdot \text{K})$ )	$C_{th}$ ( $\text{J}/(\text{K} \cdot \text{kg})$ )	$\eta$
<b><math>\text{LiTaO}_3</math></b>	1.143	0.285	43.3	-176	4.6	434	1

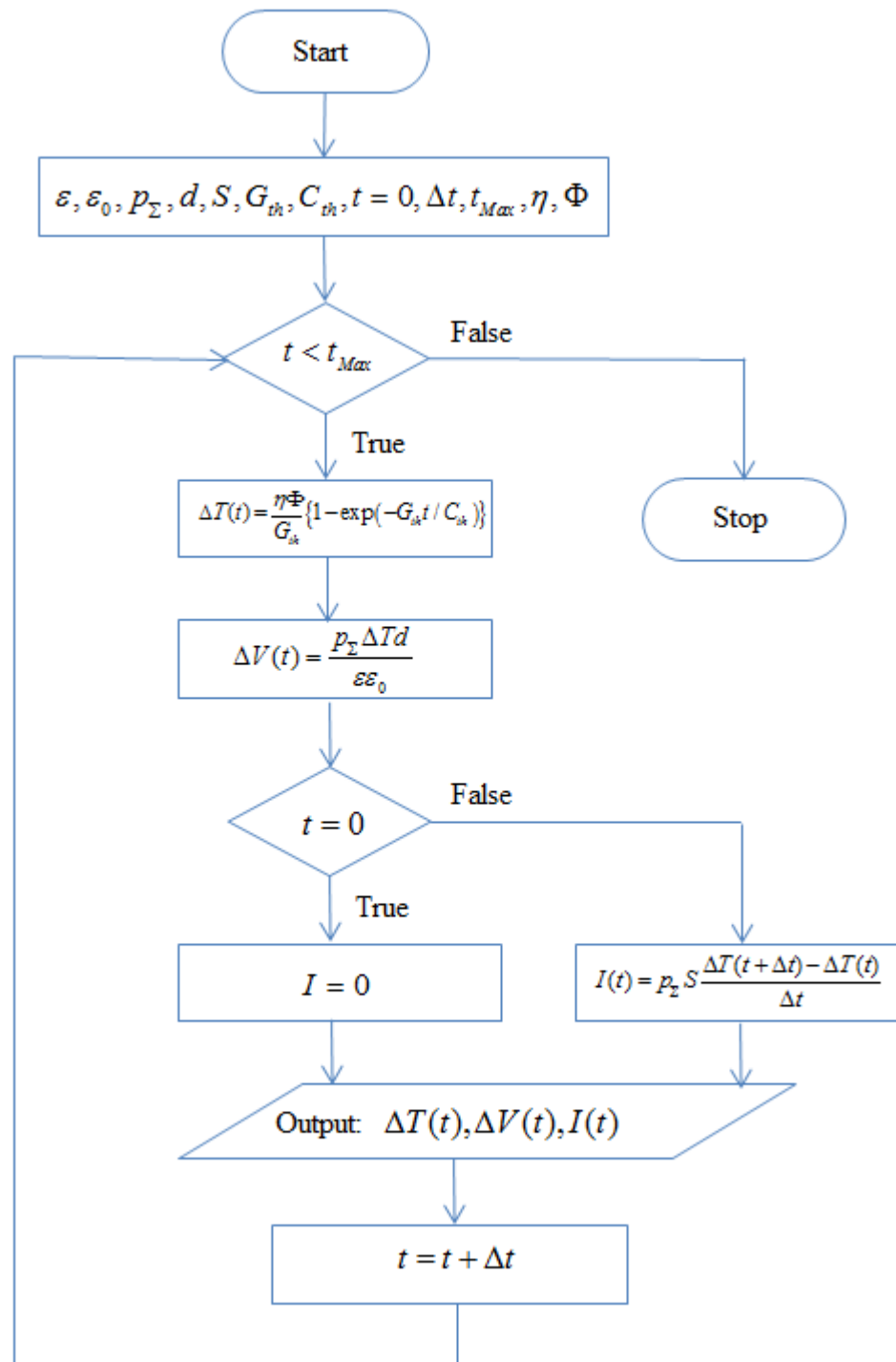


**Figure 1.** The block diagram of the piezoelectric model

### 3.1. Results

Based on the developed model of the pyroelectric detector of IR radiation, the time dependences of the temperature of the pyroelectric, as well as the voltage and current generated in this case were calculated using formulas (5), (11), (13) correspondingly and presented in Figure 2:

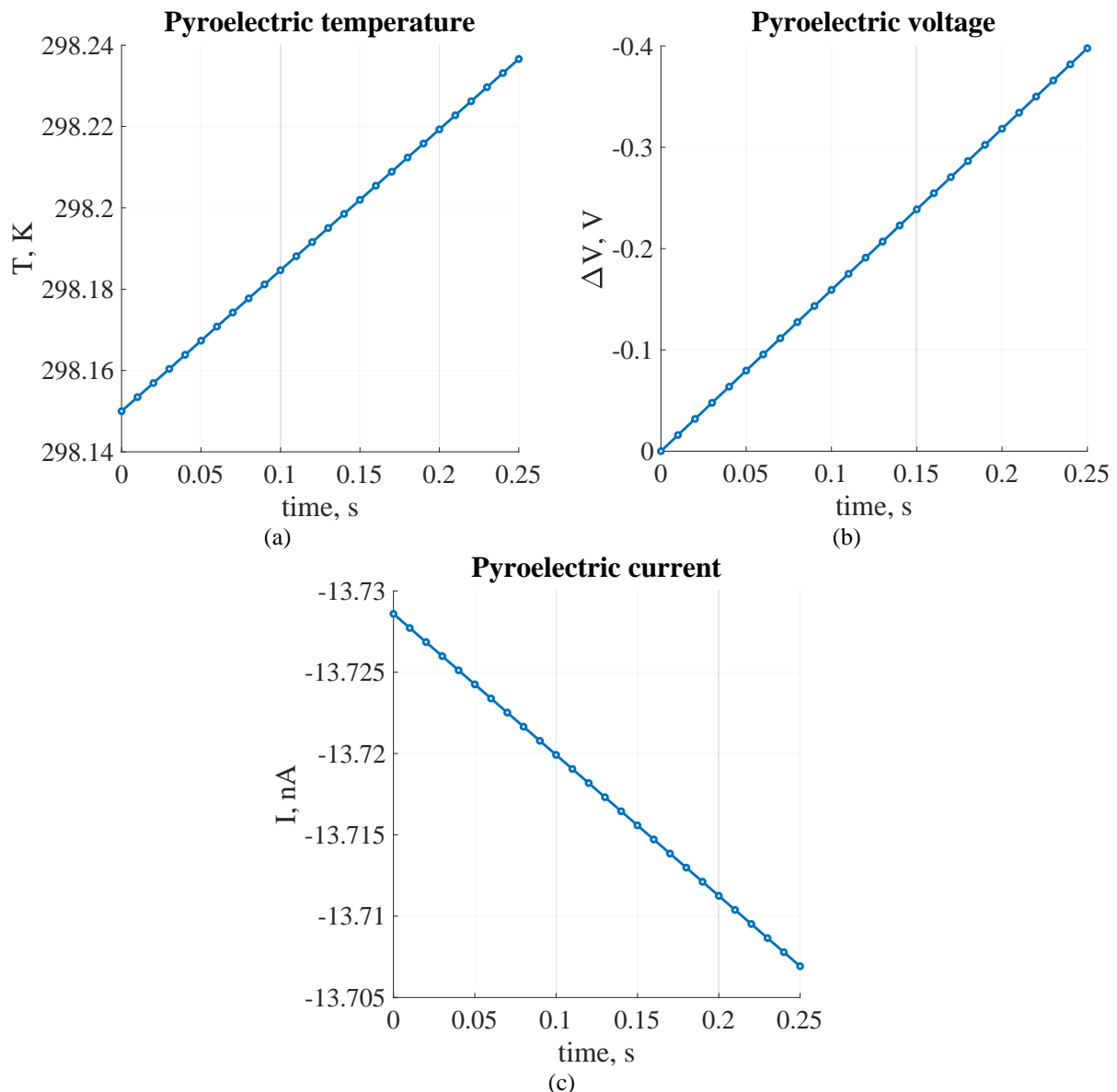


**Figure 2.** Time dependences of (a) temperature, (b) pyroelectric voltage and (c) current, obtained based on the developed model of pyroelectric thin film

From the figure presented above, it can be seen that during the time  $t = 0.25$  s the pyroelectric heated up to  $\Delta T = 80$  mK, which has led to the generation of a potential jump  $\Delta V = -0.4$  V and a the pyroelectric current  $I = -13.7$  nA.

#### 4. Conclusions

Thus, we developed a pyroelectric model using the Matlab Simulink software package [11].

This model combines theoretical concepts of pyroelectric heating with incident infrared radiation and variation of the magnitude of the spontaneous polarization vector as a function of temperature, which makes it possible to obtain time-dependent characteristics of current, voltage, and temperature of the pyroelectric thin film, respectively.

From the dependencies of the current, voltage and temperature of the pyroelectric calculated within this model, it follows that the pyroelectric current decreases and the pyroelectric surface potential increases respectively during heating of the pyroelectric thin film, as shown in Figure 2.

The results will be useful for further development of pyroelectric IR detectors.

### Acknowledgments

This research was performed using the equipment of the R&D Center «MEMSEC» (MIET), the facilities of the R&D Center «Sensorics» (MIET), and financially supported by the RF President Grant (No. 075-15-2019-1139).

### References

- [1] Vallmer M and Möllmann K-P 2010 *Infrared Thermal Imaging* (Weinheim: Wiley-VCH)
- [2] Batra A K and Aggarwal M D 2013 *Pyroelectric Materials: Infrared Detectors, Particle Accelerators and Energy Harvesters* (Washington: SPIE)
- [3] Porter S G 1981 *Ferroelectrics* **33** 193-206
- [4] Joshi J C and Dawar A L 1982 *Phys. Stat. Sol. (a)* **70** 353-369
- [5] Lang S B 2005 *Phys. Today* **58** 31-36
- [6] Bhalla A S and Newnham R E 1980 *Phys. Stat. Sol. (a)* **58** K19-K24
- [7] Putley E H 1970 The Pyroelectric Detector *Semiconductors and Semimetals (Infrared Detectors vol 5)* ed R K Willardson and A C Beer (Amsterdam: Elsevier) chapter 6 pp 259-285
- [8] Srinivasan M R 1984 *B. Mater. Sci.* **6** 317-325
- [9] Kruse P W 2001 *Uncooled Thermal Imaging Arrays Systems and Applications* (Mumbai: Springer India)
- [10] Lithium Tantalate parameters, website, <https://www.korth.de/index.php/162/items/20.html>
- [11] Matlab, Mathworks, website, <https://www.mathworks.com/products/matlab.html>